

This is the accepted manuscript made available via CHORUS. The article has been published as:

## Excitation of shear Alfvén waves by a spiraling ion beam in a large magnetoplasma

S. K. P. Tripathi, B. Van Compernelle, W. Gekelman, P. Pribyl, and W. Heidbrink

Phys. Rev. E **91**, 013109 — Published 28 January 2015

DOI: [10.1103/PhysRevE.91.013109](https://doi.org/10.1103/PhysRevE.91.013109)

# Excitation of shear Alfvén waves by a spiraling ion beam in a large magnetoplasma

S. K. P. Tripathi,<sup>1,\*</sup> B. Van Compernelle,<sup>1</sup> W. Gekelman,<sup>1</sup> P. Pribyl,<sup>1</sup> and W. Heidbrink<sup>2</sup>

<sup>1</sup>*Physics and Astronomy, University of California at Los Angeles, Los Angeles, CA 90095*

<sup>2</sup>*Physics and Astronomy, University of California at Irvine, Irvine, CA 92697*

## Abstract

Generation of shear Alfvén waves by the Doppler-shifted ion-cyclotron-resonance (DICR) of a spiraling  $H^+$  ion beam with magnetic fluctuations in a dual-species magnetized plasma with  $He^+$  and  $H^+$  ions has been investigated on the Large Plasma Device. The ambient plasma density and electron temperature were significantly enhanced by the beam. The Alfvén waves were left-handed polarized and traveled in the direction opposite to the ion beam. This is the first experimental demonstration of the DICR excitation of traveling shear Alfvén waves in a laboratory magnetoplasma.

PACS numbers: 52.35.Bj, 52.35.Qz, 94.05.Pt, 98.70.Sa

---

\* tripathi@physics.ucla.edu

## I. INTRODUCTION

Generation of Alfvén waves [1, 2] by energetic particles is a fundamental topic of interest for the controlled magnetic-fusion, laboratory, and space plasma communities. In Tokamak plasmas, Alpha-particles and fast-ions can trigger a variety of Alfvén modes and nonlinearly interact with them [3–5]. In extreme scenarios, this interaction was observed to trigger a dramatic deconfinement of energetic particles that significantly impacted the energy efficiency of the Tokamaks [6, 7]. In space plasmas, the Doppler-shifted ion-cyclotron resonance (DICR) between energetic protons and magnetic fluctuations has been postulated to isotropize the cosmic rays and affect its energy exchange with the interstellar magnetoplasma [8]. The DICR interaction of Alfvén waves with energetic ions has relevance to the low-altitude auroral zone [9], solar-wind [10], generation of the fast solar-wind [11], and scattering of energetic ions by Alfvén waves in solar-flare loops and laboratory plasmas [12, 13]. These studies were primarily focused on studying the role of Alfvén waves in affecting the transport of spiraling ions due to DICR. In addition, the occurrence of an Alfvén ion-cyclotron instability (characterized by sub-cyclotron fluctuations with  $k_{\parallel} \gg k_{\perp}$ ) associated with the anisotropy of the bulk ion distribution has drawn interest in Tandem mirror machines [14, 15]. Global and compressional Alfvén eigenmodes on Tokamaks are believed to be excited through DICR with fast-ions [16, 17], although the identification of these modes based on edge-polarization measurements are often inconclusive [18]. This letter reports new results on the generation of traveling shear Alfvén waves through DICR of a spiraling ion beam with magnetic fluctuations in an ambient magnetoplasma.

The DICR condition is governed by the equation,  $f = nf_{cb} + Sv_{b\parallel}/\lambda_{\parallel}$ , where  $f$  is the wave frequency,  $f_{cb}$  is the gyro-frequency of the beam,  $\lambda$  is the wavelength of the wave,  $v_b$  is the beam speed,  $n = \pm 1, \pm 2, \pm 3, \dots$ , and  $S$  is  $+1/-1$  for the co-/counter-propagating waves with the beam. The subscripts  $\parallel$  and  $\perp$  denote components of the physical quantities in the parallel and perpendicular directions of the equilibrium magnetic field and the subscripts  $e$ ,  $b$ ,  $1$ , and  $2$  indicate electrons, ion-beam, heavier-ion, and lighter-ion species, respectively. The experiment is conducted with a sub-Alfvénic  $H^+$  beam in a dual species plasma with  $He^+$  (gyro-frequency  $f_{ci1}$ ) and  $H^+$  (gyro-frequency  $f_{ci2}$ ) ions. The DICR and Landau resonance (LR) conditions can be expressed in terms of the cyclotron resonance function  $C$  and the Landau resonance function  $L$  as,

$$C = \frac{f}{f_{cb}} \left( 1 - \frac{Sv_{b\parallel}}{v_{\phi\parallel}} \right), \quad (1)$$

$$L = \frac{v_{b\parallel}}{v_{\phi\parallel}}, \quad (2)$$

where  $v_{\phi}$  is the phase speed of the wave and is a function of frequency and ambient plasma parameters. The DICR and LR conditions are satisfied, when  $C = n$  and  $L = 1$ , respectively. The dispersion relation of shear Alfvén waves with a small perpendicular wavelength [ $\lambda_{\perp} < L_j = c/(2\pi f_{pj})$ ] in a two ion-species plasma is given by [19],

$$k_{\parallel} = k_0 \sqrt{\epsilon_{\perp}} \left[ 1 - k_{\perp}^2 / (k_0^2 \epsilon_{\parallel}) \right]^{1/2}, \quad (3)$$

where  $k_0 = 2\pi f/c$ ,  $c$  is the speed of light,  $k$  is the wave number,  $L_j$  is the ion inertial length, and  $\epsilon$  is the dielectric tensor. For a multi-species cold-plasma,  $\epsilon_{\perp} = 1 - \sum_j f_{pj}^2 / (f^2 - f_{cj}^2)$  and  $\epsilon_{\parallel} = 1 - \sum_j f_{pj}^2 / f^2$ , where  $f_{pj}$  is the plasma frequency,  $f_{cj}$  is the gyro-frequency, and

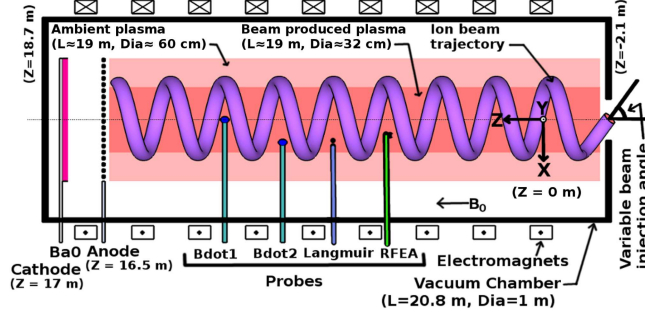


FIG. 1. (Color online) Schematic of the ion-beam experiment on the Large Plasma Device showing the cylindrical vacuum chamber, electromagnets, ambient magnetoplasma produced by the BaO cathode, helical trajectory of the beam, the beam-produced plasma, diagnostic probes, and the  $xyz$  coordinate system. The schematic depicts the top cross-sectional view of the device and is not drawn to the scale.

index  $j$  spans over electrons and ion-species. The dispersion relation permits propagation of Alfvén waves in two frequency bands, (i) the lower frequency band ( $f < f_{ci1}$ ) and (ii) the upper frequency band ( $f_{ii} < f < f_{ci2}$ ), where  $f_{ii} = \sqrt{(f_{p1}^2 f_{c2}^2 + f_{p2}^2 f_{c1}^2) / (f_{p1}^2 + f_{p2}^2)}$  is the ion-ion hybrid frequency. The role of the DICR and LR processes in generating the shear Alfvén waves can be examined for given plasma parameters by estimating the parallel phase speed from Eq. (3) and substituting it in Eqs. (1) and (2). Alfvén waves have small but finite parallel electric field [2], hence, they can grow due to inverse Landau damping when  $L \gtrsim 1$ . For the growth of the Alfvén waves due to DICR,  $C \lesssim 1$ , the waves must have appropriate polarization (e.g., left-handed for  $n > 0$  and sub-Alfvénic beams), and the beam intensity should be adequate to compensate for the damping of the waves.

## II. EXPERIMENTAL SETUP

The experiment was conducted on the Large Plasma Device (LAPD) which produces a 19 m long, 60 cm diameter cylindrical magnetoplasma with 10 - 20 ms pulse-width and 1 Hz repetition rate using a barium-oxide coated hot cathode [20, 21]. The schematic of the experiment is shown in Fig. 1. The He and H<sub>2</sub> gas pressures were 0.08 mTorr and 0.03 mTorr, respectively. The ambient magnetic field  $B_0$  was 1800 G and the plasma was current-free. The H<sup>+</sup> ion beam ( $E_b = 15$  keV,  $I_b = 10$  A, divergence  $< 1.5^\circ$ , pulse-width = 800  $\mu$ s,  $v_b = 1.69 \times 10^6$  m/s) was injected from the side opposite to the plasma source of the LAPD with 1/3 Hz repetition rate. The beam was produced using the upgraded LAPD ion source [22] that utilizes a LaB<sub>6</sub> plasma source [23] and produces a quiescent ion-beam. A Cartesian coordinate system (see Fig. 1) is used to present the results.

The H<sup>+</sup> beam ( $f_{cb} = 2.74$  MHz, gyro-radius  $r_b = 7.8$  cm,  $v_{b\parallel}/v_{b\perp} = 0.75$ ,  $\Delta z$  between neighboring orbits = 37.2 cm, number of orbits = 51) is shown schematically in Fig. 1. The beam spirals down the ambient plasma with a  $53^\circ$  pitch angle  $\theta_p$  and produces additional plasma. The interaction between the beam and the ambient plasma is explored using Langmuir probes, three-axis magnetic-loop probes, and retarding field energy analyzers (RFEA) [22]. These probes were mounted on the radial ports at multiple  $z$ -locations and moved in  $xy$  planes using automated probe drives to record the data.

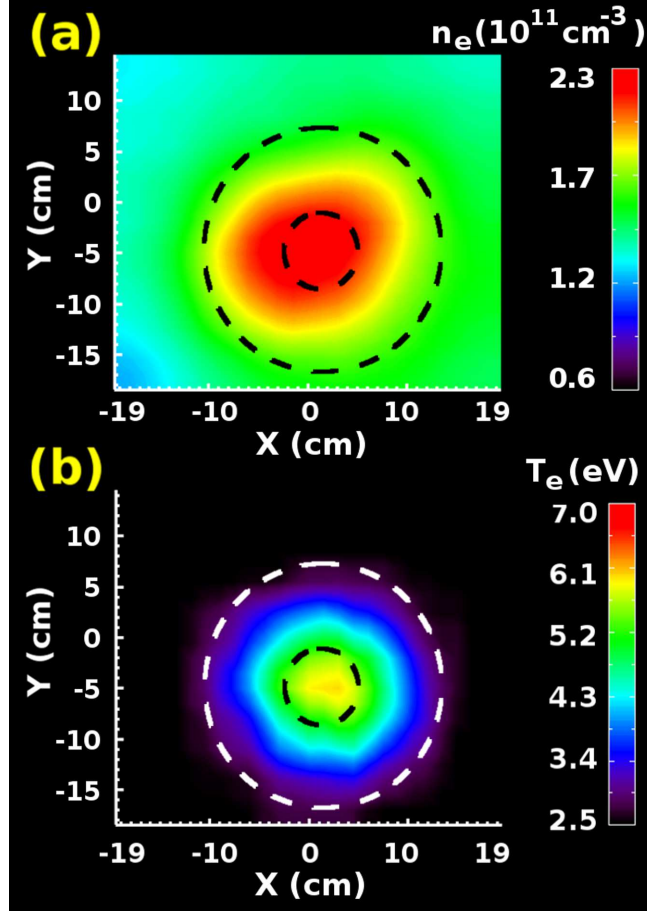


FIG. 2. (Color online) Electron plasma density (a) and electron temperature (b) profiles of the  $\text{H}^+$  beam produced plasma at  $z = 9.59$  m in the LAPD. The beam was injected at 50 ms into the afterglow plasma and profiles were recorded  $630 \mu\text{s}$  after the beam was turned on. The radial extent of the beam-orbit is indicated by circular-dotted lines.

### III. RESULTS AND DISCUSSIONS

The electron plasma density  $n_e$  and temperature  $T_e$  profiles of the ambient plasma were recorded using a swept Langmuir probe calibrated by a microwave-interferometer. The ion beam was injected at 50 ms in the plasma afterglow. Plasma-formation by the beam occurred during the first  $400 \mu\text{s}$  of the  $800 \mu\text{s}$  beam-pulse. During initial  $200 \mu\text{s}$  of the plasma-formation,  $T_e$  increased from  $0.2 \pm 0.1$  eV to  $5.0 \pm 1.0$  eV. This was followed by 2–3 times increase in  $n_e$  within  $200 \mu\text{s}$ . The  $n_e$  and  $T_e$  profiles remained nearly unchanged during the second-half of the beam pulse. Typical profiles of  $n_e$  and  $T_e$  were measured during this steady-state phase and displayed in Fig. 2. Plasma production by the ion beam cannot be explained by the direct ionization of neutrals by the beam, since the associated ionization mean-free-paths (92–600 m) are larger than the length of the beam trajectory in the LAPD ( $\approx 44$  m). Initial estimates indicate that the  $\text{H}^+$  beam-assisted plasma production is a two-step process [24] which involves significant heating of the electrons and ionization of neutrals by electrons in the tail of the heated distribution.

The profiles of the current-density of the ion-beam were recorded at two axial locations

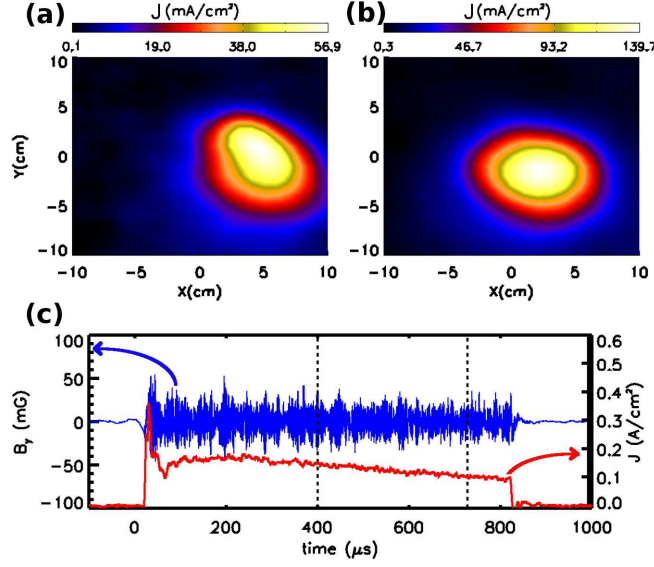


FIG. 3. (Color online) Profiles of a 15 kV  $H^+$  beam with 10 A current at two axial locations, (a)  $z = 13.42$  m and (b)  $z = 0.64$  m in the LAPD plasma recorded using a retarding field energy analyzer. (c) Typical time traces of the ion beam pulse from the analyzer (at  $x=2.0$  cm,  $y=-1.0$  cm,  $z=0.64$  m) and beam-driven magnetic-fluctuations (at  $x=0$  cm,  $y=0$  cm,  $z=3.83$  m) are indicated by the red (lower) and blue (upper) traces associated with the right and left axes, respectively.

[see Fig. 3(a) and 3(b)] in the ambient plasma using a RFEA oriented to maximize the beam signal at each axial location. The RFEA was designed to detect the incoming fast-ions ( $E > 84$  eV) within a  $20^\circ$  acceptance-cone angle. The  $H^+$  ions that underwent large pitch-angle-scattering ( $\theta_p < 43^\circ$  and  $\theta_p > 63^\circ$ ) were not collected by the RFEA. The size of the beam spot in both profiles is comparable to the size of the beam-extractor-grids in the ion source. The peak  $H^+$  beam-density  $n_b$  was  $5 \times 10^9 \text{ cm}^{-3}$  at  $z = 0.64$  m (near the entrance in the LAPD plasma) and  $2 \times 10^9 \text{ cm}^{-3}$  at  $z = 13.42$  m. Estimates based on these profile measurements and charge-exchange cross-sections [25] for  $H^+ \rightarrow H$  and  $H^+ \rightarrow He$  indicate  $50 \pm 5$  % of the beam-ions were lost in traversing the 12.8 m axial distance by the charge exchange and  $10 \pm 5$  % of the beam-ions were scattered out of the acceptance-cone of the RFEA. The time evolution of the typical beam signal (recorded by the RFEA) and beam-driven magnetic-fluctuations (measured using a magnetic-loop probe with a 3.0 MHz low-pass-filter) are displayed in Fig. 3(c). The high-frequency waves (e.g., beam-driven lower-hybrid and whistler waves with  $f > f_{ci2}$ ) were filtered out. The beam is expected to take  $\approx 18.6 \mu\text{s}$  to travel through the plasma. The delayed arrival of the beam-pulse at multiple  $z$ -locations was measured and found to be consistent with the expected time-of-flight of the  $H^+$  ion beam with  $v_{b||} = 1.02 \times 10^6$  m/s.

Amplitude spectra of magnetic fluctuations in the ambient plasma were recorded in the presence and absence of the beam and are plotted in Fig. 4. The spectra were produced by averaging over the Fourier-transforms of 15015 time-traces of  $B_y$  fluctuations. The time-traces (duration =  $328 \mu\text{s}$ , sampling-rate = 100 MHz) were acquired using a fixed magnetic-loop probe at  $x=0$  cm,  $y=-2$  cm, and  $z=7.67$  m on the shot-to-shot basis under nearly identical experimental conditions. The time-range of the data for generating the “BEAM ON” spectra is indicated by the vertical-dotted lines in Fig. 3(c). The time-series for the

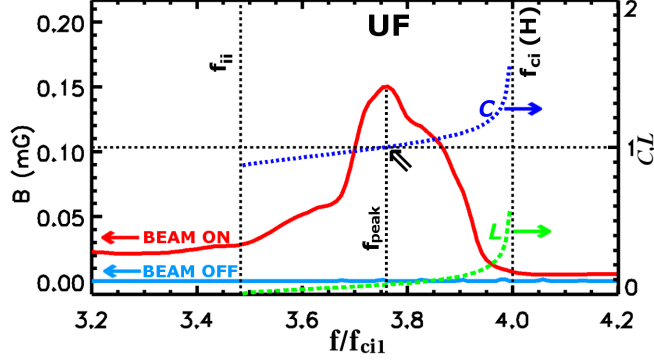


FIG. 4. (Color online) In the presence of the  $H^+$  beam, amplification of magnetic fluctuations of the ambient plasma (8%  $H^+$  and 92%  $He^+$ ,  $f_{ci1} = 685$  kHz) is depicted. The red and blue curves (labeled as BEAM ON and BEAM OFF, y-axis on the left as shown by the left-arrows) are the spectra of magnetic fluctuations in the presence and absence of the beam, respectively. The “beam on” spectra peaks at  $f_{peak}$ . The dotted-blue (labeled by C) and dashed-green (labeled by L) curves (y-axis on the right as indicated by the right-arrows) are the cyclotron and Landau resonance functions, respectively. The resonance conditions are satisfied at a frequency where C or L curves intersect the horizontal-dotted line. The  $n = 1$  DICR condition is satisfied (marked by the double-arrow) near  $f_{peak}$  suggesting the excitation of shear Alfvén waves through DICR of the ion beam.

“BEAM OFF” spectra were acquired 320  $\mu s$  after turning off the beam. In the presence of the beam, magnetic fluctuations were amplified by  $\approx 40$  times in the lower frequency band ( $f < f_{ci1}$ ) and  $\approx 200$  times in the upper frequency band ( $f_{ii} < f < f_{ci2}$ , labeled as UF in Fig. 4). The amplification was dominant in the upper frequency band and is the focus of this letter.

For our experimental parameters, average  $n_e = 1.5 \times 10^{11} \text{ cm}^{-3}$ ,  $T_e = 5.0 \text{ eV}$ ,  $f_{ci1} = 685$  kHz,  $f_b = f_{ci2} = 4f_{ci1} = 2740$  kHz, Alfvén speed  $v_A = 5.2 \times 10^6 \text{ m/s}$ , and electron thermal speed  $v_{the} = 9.4 \times 10^5 \text{ m/s}$ . Here,  $v_{the}/v_A = 0.18$  and  $v_{b\parallel}/v_A = 0.20$ , hence the beam is sub-Alfvénic and Alfvén waves are in the inertial regime. By identifying the ion-ion hybrid frequency ( $f_{ii} = 2385$  kHz), the relative concentration of  $He^+$  ( $n_1 = 0.92n_e$ ) and  $H^+$  ( $n_2 = 0.08n_e$ ) ions was estimated [19] and used in determining the  $v_A$ . For the excitation of Alfvén waves ( $f < f_{ci2} = f_{cb}$ ) through the DICR process by a sub-Alfvénic ion beam, Eq. (1) requires  $S = -1$ . This implies that the wave must propagate in the opposite direction to the beam. Using these parameters in Eqs. (1–3),  $C(f)$  and  $L(f)$  were evaluated and plotted in Fig. 4. The LR and  $n = 1$  DICR resonances are expected to occur at a frequency where associated resonance functions are equal to 1, i.e. where they cross the horizontal dotted-line. The results indicate that the LR and  $n > 1$  DICR can occur only at  $f_{ci1}$  and  $f_{ci2}$ , where the wave signal is negligible. However, the  $n = 1$  DICR condition is satisfied near  $f_{peak}$  in Fig. 4 where maximum amplitude of Alfvén waves is detected. This implies that the waves in the UF band are generated by the  $n = 1$  DICR process. The counter-propagation of the wave with the beam and the mode-structure of the wave is discussed below.

A cross-spectral data analysis technique [26], which required a fixed-movable probe pair, was used to derive the mode structure of waves at different frequencies. This technique is efficient in identifying the mode-structure in a plasma where a multitude of waves exist. In addition to the fixed magnetic-loop probe, a three-axis magnetic-loop probe ( $z = 8.63 \text{ m}$ )



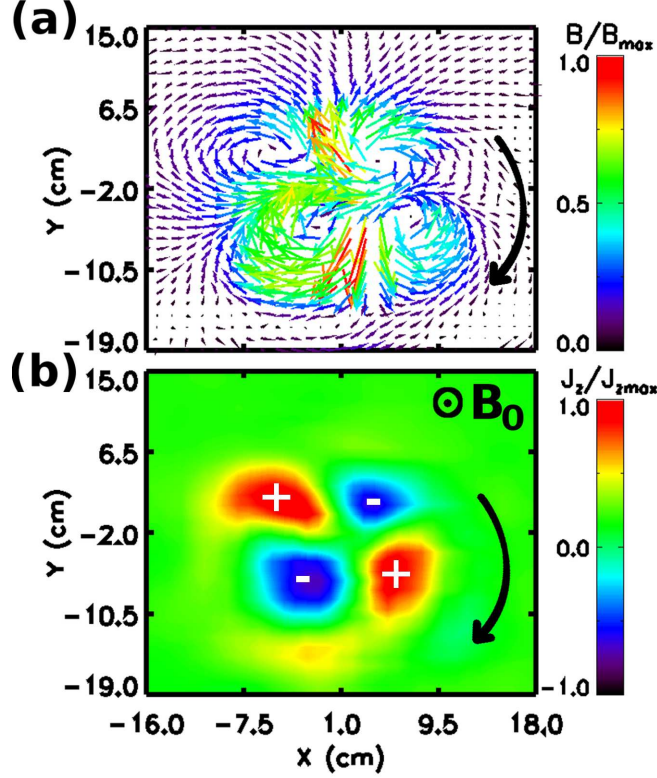


FIG. 5. (Color online) The structure of the (a) wave magnetic field and (b) associated axial current-density in the high frequency band at  $f/f_{ci1} = 3.67$  ( $f = 2516$  kHz,  $\Delta f = 24$  kHz). The  $n = 1$  Doppler-shifted cyclotron resonance condition is satisfied near this frequency. Directions of the ambient magnetic field  $B_0$  and rotation of the structure are indicated by the circled-dot and arrows, respectively. Positive and negative axial current-densities are marked by + and - in the bottom panel and better viewed in the color online figure using the associated color scale. The Alfvén wave has a left-handed polarization and grows by extracting the perpendicular energy from the spiraling ion beam.

was moved in a  $34 \times 34$  cm  $xy$  plane with  $\Delta x = \Delta y = 1.0$  cm. At every spatial-location in the plane, 11 time-traces were recorded by the movable-probe and data from the fixed probe were acquired simultaneously. The ensemble-averaged phases of  $B_{x,y,z}(x, y)$  wave-field-components in the plane were retrieved relative to the phase of  $B_y$  wave-field-component at the fixed-probe location. Using this relative phase and amplitude in the plane, mode-structures of the waves were generated at different frequencies. The mode-structure at  $f/f_{ci1} = 3.67$  is depicted in Fig. 5 by showing the magnetic-field vectors in the top panel and associated axial current-density  $J_z$  in the bottom panel. The counter-propagation of the wave with  $v_{\phi\parallel}/v_A = 2.96$  ( $\lambda_{\parallel} \approx 6$  m,  $S = -1$ ) was verified. The dispersion relation in Eq. (3), estimates  $v_{\phi\parallel}/v_A = 2.85$  at this frequency in close agreement with the measurements. These observations justify the use of Eq. (3) and  $S = -1$  in estimating the  $C(f)$  displayed in Fig. 4. The direction of the rotation of the wave-pattern in Fig. 5 shows the wave is left-handed (LH) polarized with  $m = 2$  azimuthal mode number. This is consistent with the LH rotation of the vectors in the core, where the wave intensity is maximum. The wave in the UF band satisfies the dispersion relation of shear Alfvén waves, exists below  $f_{ci2}$ , has



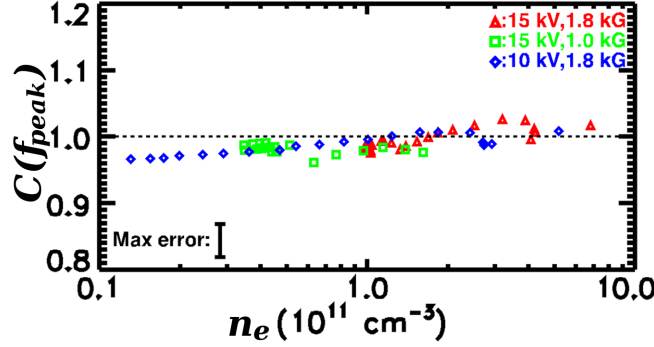


FIG. 6. (Color online) The value of the cyclotron resonance function  $C(f_{peak})$  was estimated at different  $f_{peak}$ 's (see Fig. 4) and plotted against  $n_e$ .  $f_{peak}$  was indirectly varied by changing  $n_e$ ,  $E_b$ , and  $B_0$ . The results evince  $C(f_{peak}) = 1.00 \pm 0.04$  over a broad range of parameters, hence confirm the role of the  $n = 1$  DICR process in exciting the shear Alfvén wave.

LH polarization, and negligible  $B_z$  fluctuations ( $B_z/B_{x,y} < 0.1$ ). These observations suggest the DICR excitation of shear Alfvén waves in the UF band by the ion beam.

To further examine the role of DICR in destabilizing shear Alfvén waves, spectra of magnetic-fluctuations were recorded in the presence of the beam under 100 different conditions. These conditions were arranged by varying  $n_e$ , beam energy  $E_b$ , and  $B_0$ . Plasma density decays in the afterglow, hence  $n_e$  was varied by injecting the beam at 34 different times in the afterglow of the Ba0-cathode produced plasma. For each condition,  $f_{peak}$  (frequency where “beam on” spectra peaks in the UF band) and the value of  $C(f)$  at  $f = f_{peak}$  were calculated by substituting the measured parameters in Eqs. (1) and (3). The main source of the error in estimates of  $C(f_{peak})$  is the systematic error in the determination of  $n_e$  from Langmuir probe measurements. The maximum error and dependence of  $C(f_{peak})$  on  $n_e$ ,  $B_0$ , and  $E_b$  are displayed in Fig. 6. The results evince that maxima of the “beam on” fluctuation-spectra appear at a frequency where  $C \approx 1$ . This confirms the excitation of shear Alfvén waves through the  $n = 1$  DICR of the spiraling ion-beam over a broad range of parameters.

#### IV. SUMMARY

In summary, generation of shear Alfvén waves through Doppler-shifted cyclotron resonance of a spiraling ion beam with magnetic fluctuations in a large magnetoplasma has been demonstrated. Details of the interaction were examined by estimating the Landau and Cyclotron resonance functions, recording the LH polarization of the wave at the DICR frequency, and confirming the counter-propagation of the wave with the beam. The Alfvén wave generation by DICR can play important roles in exciting sub-cyclotron fluctuations in a variety of laboratory and space plasmas.

Our future research will be targeted toward further exploring the physics of energetic-ion interactions with magnetized plasmas – especially on investigating the role of nonresonant processes in destabilizing the Alfvén waves, electron-heating and plasma production by an ion-beam, excitation of whistler and lower hybrid waves by the beam, and scattering of the fast-ions of the beam by the Alfvén waves.

## ACKNOWLEDGMENTS

The authors acknowledge valuable assistance in the fabrication of the ion source from Z. Lucky and M. Drandell, and thank S. Vincena, G. J. Morales, T. A. Carter, B. Breizman, H. Boehmer, and N. Crocker for helpful discussions. The research was performed at the Basic Plasma Science Facility, UCLA, which is jointly funded by NSF and DOE.

- 
- [1] H. Alfvén, *Nature (London)* **150**, 405 (1942).
  - [2] W. Gekelman, S. Vincena, B. Van Compernelle, G. J. Morales, J. E. Maggs, P. Pribyl, and T. A. Carter, *Phys. Plasmas* **18**, 055501 (2011).
  - [3] M. N. Rosenbluth and P. H. Rutherford, *Phys. Rev. Lett.* **34**, 1428 (1975).
  - [4] W. W. Heidbrink, *Phys. Plasmas* **15**, 055501 (2008).
  - [5] K.-L. Wong, *Plasma Phys. Controlled Fusion* **41**, R1 (1999).
  - [6] H. Duong, W. Heidbrink, E. Strait, T. Petrie, R. Lee, R. Moyer, and J. Watkins, *Nucl. Fusion* **33**, 749 (1993).
  - [7] R. B. White, E. Fredrickson, D. Darrow, M. Zarnstorff, R. Wilson, S. Zweben, K. Hill, Y. Chen, and G. Fu, *Phys. Plasmas* **2**, 2871 (1995).
  - [8] E. G. Zweibel, *Phys. Plasmas* **20**, 055501 (2013).
  - [9] R. L. Lysak and M. A. Temerin, *Geophys. Res. Lett.* **10**, 643 (1983).
  - [10] J. Araneda, H. Astudillo, and E. Marsch, *Space Sci. Rev.* **172**, 361 (2012).
  - [11] J. V. Hollweg and P. A. Isenberg, *J. Geophys. Res.: Space Phys.* **107**, SSH 12 (2002).
  - [12] D. H. Tamres, D. B. Melrose, and R. C. Canfield, *Astrophys. J.* **342**, 576 (1989).
  - [13] Y. Zhang, W. W. Heidbrink, S. Zhou, H. Boehmer, R. McWilliams, T. A. Carter, S. Vincena, and M. K. Lilley, *Phys. Plasmas* **16**, 055706 (2009).
  - [14] T. A. Casper and G. R. Smith, *Phys. Rev. Lett.* **48**, 1015 (1982).
  - [15] J. D. Hanson and E. Ott, *Phys. Fluids* **27**, 150 (1984).
  - [16] N. Gorelenkov, E. Fredrickson, E. Belova, C. Cheng, D. Gates, S. Kaye, and R. White, *Nucl. Fusion* **43**, 228 (2003).
  - [17] N. Crocker, E. Fredrickson, N. Gorelenkov, W. Peebles, S. Kubota, R. Bell, A. Diallo, B. LeBlanc, J. Menard, M. Podest, K. Tritz, and H. Yuh, *Nucl. Fusion* **53**, 043017 (2013).
  - [18] E. Fredrickson, N. Gorelenkov, E. Belova, N. Crocker, S. Kubota, G. Kramer, B. LeBlanc, R. Bell, M. Podesta, H. Yuh, and F. Levinton, *Nucl. Fusion* **52**, 043001 (2012).
  - [19] S. T. Vincena, W. A. Farmer, J. E. Maggs, and G. J. Morales, *Phys. Plasmas* **20**, 012111 (2013).
  - [20] D. Leneman, W. Gekelman, and J. Maggs, *Rev. Sci. Instrum.* **77**, 015108 (2006).
  - [21] W. Gekelman, H. Pfister, Z. Lucky, J. Bamber, D. Leneman, and J. Maggs, *Rev. Sci. Instrum.* **62**, 2875 (1991).
  - [22] S. K. P. Tripathi, P. Pribyl, and W. Gekelman, *Rev. Sci. Instrum.* **82**, 093501 (2011).
  - [23] B. Van Compernelle, W. Gekelman, P. Pribyl, and C. M. Cooper, *Phys. Plasmas* **18**, 123501 (2011).
  - [24] W. Ott, E. Speth, and the W7-AS Team, *Nucl. Fusion* **42**, 796 (2002).
  - [25] C. F. Barnett and H. K. Reynolds, *Phys. Rev.* **109**, 355 (1958).
  - [26] D. E. Smith, E. Powers, and G. S. Caldwell, *IEEE Trans. Plasma Sci.* **2**, 261 (1974).